ACS Infectious Diseases

Article

Cite This: ACS Infect. Dis. 2020, 6, 237−249

pubs.acs.org/journal/aidcbc

Exploiting Correlations between Protein Abundance and the Functional Status of *saeRS* and *sarA* To Identify Virulence Factors of Potential Importance in the Pathogenesis of *Staphylococcus aureus* Osteomyelitis

Aura M. Ramirez,[†] Stephanie D. Byrum,[‡,§] Karen E. Beenken,[†] Charity Washam,[‡,§] Rick D. Edmondson,[‡] Samuel G. Mackintosh,[‡] Horace J. Spencer,[∥] Alan J. Tackett,[‡,§] and Mark S. Smeltzer*[,†,⊥]

[†]Department of Microbiology and Immunology, College of Medicine, University of Arkansas for Medical Sciences, 4301 W. Markham Street, Slot 511, Little Rock, Arkansas 72205, United States

[‡]Department of Biochemistry and Molecular Biology, University of Arkansas for Medical Sciences, 4301 W. Markham Street, Slot 516, Little Rock, Arkansas 72205, United States

[§]Arkansas Children's Research Institute, 1 Children's Way, Little Rock, Arkansas 72202, United States

[∥]Department of Biostatistics, University of Arkansas for Medical Sciences, 4301 W. Markham Street, Little Rock, Arkansas 72205, United States

[⊥]Department of Orthopaedic Surgery, University of Arkansas for Medical Sciences, 4301 W. Markham Street, Slot 531, Little Rock, Arkansas 72205, United States

Supporting Information

ABSTRACT: We used a murine model of postsurgical osteomyelitis (OM) to evaluate the relative virulence of the *Staphylococcus aureus* strain LAC and five isogenic variants that differ in the functional status of *saeRS* and *sarA* relative to each other. LAC and a variant in which *saeRS* activity is increased (*sae*^{C}) were comparably virulent to each other, while Δ*saeRS*, Δ*sarA*, Δ*saeRS*/Δ*sarA*, and *sae*^{C}/Δ*sarA* mutants were all attenuated to a comparable degree. Phenotypic comparisons including a mass-based proteomics approach that allowed us to assess the number and abundance of full-length proteins suggested that mutation of *saeRS* attenuates virulence in our OM model owing primarily to the decreased production of *S. aureus* virulence factors, while mutation of *sarA* does so owing to protease-mediated degradation of these same virulence factors. This was confirmed by demonstrating that eliminating protease production restored virulence to a greater extent in a LAC *sarA* mutant than in the isogenic *saeRS* mutant. Irrespective of the mechanism involved, mutation of *saeRS* or *sarA* was shown to result in reduced accumulation of virulence factors of potential importance. Thus, using our proteomics approach we correlated the abundance of specific proteins with virulence in these six strains and identified 14 proteins that were present in a significantly increased amount ($\log_2 \geq 5.0$) in both virulent strains by comparison to all four attenuated strains. We examined biofilm formation and virulence in our OM model using a LAC mutant unable to produce one of these 14 proteins, specifically staphylocoagulase. The results confirmed that mutation of *coa* limits biofilm formation and, to a lesser extent, virulence in our OM model, although in both cases the limitation was reduced by comparison to the isogenic *sarA* mutant.

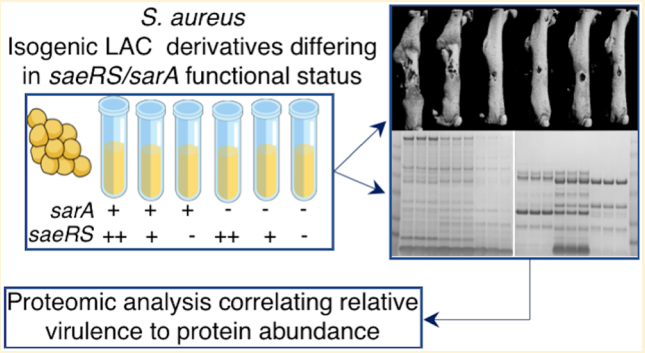

KEYWORDS: *Staphylococcus aureus, osteomyelitis, virulence factors, biofilm, protease, proteomics*

Staphylococcus aureus is the principal cause of osteomyelitis (OM) and other forms of orthopedic infection including those associated with the presence of an indwelling prosthesis. The medical treatment of these infections is complicated by a compromised localized vasculature, the presence of a biofilm, and the presence of bacterial variants (e.g., persister cells) with reduced metabolic activity and consequently increased antibiotic tolerance.[1] The continued emergence of antibiotic resistant strains, most notably methicillin-resistant *S. aureus* (MRSA), further complicates the success of traditional antibiotic-based therapies.[1] For these reasons, the majority of

Received: August 2, 2019
Published: November 13, 2019

DOI: 10.1021/acsinfecdis.9b00291
ACS Infect. Dis. 2020, 6, 237−249

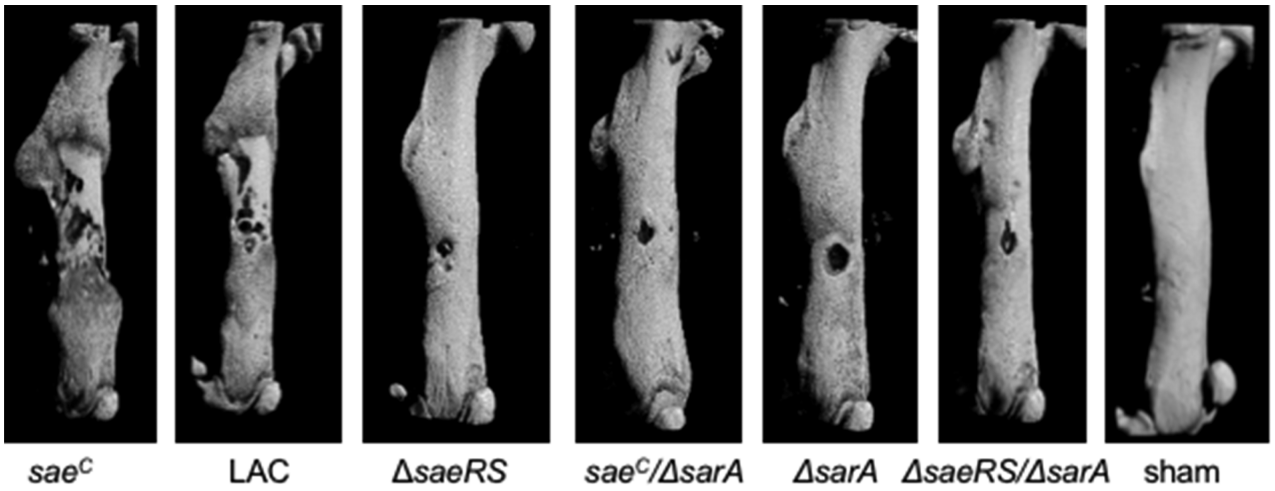

Figure 1. Impact of the functional status of *saeRS* and *sarA* in post-traumatic osteomyelitis. A murine model of post-traumatic osteomyelitis was used to assess the relative virulence of LAC, its *sarA* mutant (Δ*sarA*), and isogenic derivatives of each of these strain in which *saeRS* was either mutated (Δ*sae*) or exhibited enhanced activity (*sae*^{C}). Bones were imaged by μCT 14 days after initiation of the infection. The sham was subjected to the surgical procedure in the absence of infection. Representative images are shown from mice in each experimental group of these seven experimental groups.

OM cases caused by *S. aureus* require surgical intervention in addition to long-term, intensive antibiotic therapy.[2] Even after such intensive medical and surgical intervention the recurrence rate remains unacceptably high.[1] Identifying critical *S. aureus* virulence factors, and improving our understanding of how these factors impact pathogenesis in OM, is key to potentially finding new therapeutic targets that can be exploited to better address this clinical problem.

One approach to identifying such virulence factors is to exploit the impact of regulatory loci in the specific context of the pathogenesis of OM. Regulatory circuits in *S. aureus* are complex and highly interactive, thus allowing the bacterium to adjust the production of its many virulence factors to diverse microenvironments within the host.[3] In the specific case of OM, it has been demonstrated that mutation of the staphylococcal accessory regulator (*sarA*) or the *S. aureus* exoprotein (*saeRS*) regulatory locus attenuates virulence in a murine model of postsurgical OM as assessed by both cortical bone loss and reactive bone (callus) formation.[4,5] Mutation of both loci has also been shown to result in the increased production of extracellular proteases and decreased accumulation of specific virulence factors including alpha toxin, phenol-soluble modulins (PSMs) and protein A (Spa).[5−9] In fact, the increased production of extracellular proteases, specifically aureolysin, has been shown to play a significant role in defining the attenuation of a LAC *saeRS* mutant owing to the decreased accumulation of PSMs.[6]

Mutation of *sarA* also results in reduced accumulation of PSMs owing to protease-mediated degradation, and in fact mutation of *sarA* results in a much greater increase in protease production than mutation of *saeRS*.[7−9] This suggests that mutation of *sarA* may attenuate the virulence of LAC to an even greater extent than mutation of *saeRS*. However, the accumulation of any protein is a function of its production vs its degradation, and our studies suggest that the primary impact of mutating *saeRS* on virulence is due to reduced production of *S. aureus* virulence factors, while that of mutating *sarA* is due to protease-mediated degradation of these virulence factors.[7,8] Thus, the relative impact of these two regulatory loci in the context of OM remains unknown. To assess this experimentally, we evaluated the virulence of LAC and five isogenic derivatives that differ with respect to the functional status of *saeRS* and *sarA* relative to each other. Comparisons were made using a murine model of postsurgical OM.[4,5] We then took advantage of the results of these studies to identify and prioritize specific virulence factors of potential relevance by correlating relative virulence with the accumulation of full-length proteins present in conditioned medium (CM) from stationary phase cultures of the same strains.

RESULTS

Mutation of *saeRS* or *sarA* Attenuates the Virulence of LAC in OM to a Comparable Degree. We previously generated five derivatives of LAC that vary with respect to the functional status of *saeRS* and *sarA* relative to each other.[6,7] To assess the relative virulence of these strains, we employed a murine model of postsurgical osteomyelitis.[4,5] Briefly, a unicortical defect was created in the femur of mice. LAC or one of these five isogenic derivatives was then inoculated directly into the medullary canal. After 14 days, infected bones were harvested and analyzed by microcomputed tomography (μCT). Duplicate samples were also harvested and processed to determine bacterial burdens in the femur. By comparison to uninfected mice subjected to the same surgical procedure (sham), the femurs of all infected mice showed marked callus formation adjacent to the inoculation site and extending to the proximal and distal ends of the femur (Figure 1). In sham mice, the unicortical defect was almost completely sealed, while this was not the case with any of the infected mice irrespective of the strain used to initiate the infection.

To quantitatively assess virulence differences between these strains, μCT images were analyzed to assess relative levels of callus formation and cortical bone destruction. As assessed based on both parameters, LAC and its derivative with increased activation of *saeRS* (*sae*^{C}) were comparably virulent (Figure 2). As previously reported,[4,5] mutation of *saeRS* (Δ*saeRS*) and/or *sarA* (Δ*sarA*) resulted in decreased callus formation and cortical bone destruction. The functional status of *saeRS* did not have a statistically significant effect in the *sarA* mutant with respect to either of these parameters, but there did

DOI: 10.1021/acsinfecdis.9b00291
ACS Infect. Dis. 2020, 6, 237−249

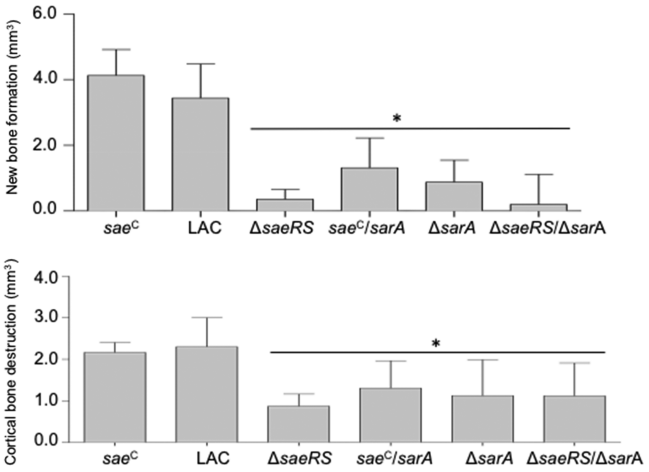

Figure 2. Quantitative assessment of reactive bone formation and cortical bone destruction as a function of *saeRS* and *sarA*. Analysis of μCT images was used to assess reactive new bone formation (top) and cortical bone destruction (bottom) in each of 5 mice infected with the indicated strains. Statistical analysis was done by one-way ANOVA with Dunnett's correction. Asterisk (*) indicates a significant difference relative to LAC.

appear to be a trend suggesting that reactive bone formation decreased as the combined activity of both *sae* and *sarA* decreased (Figure 2). Similarly, while the difference did not reach statistical significance, mutation of *saeRS* appeared to limit callus formation to a greater extent than mutation of *sarA*.

In addition to μCT analysis, we also quantified bacterial burdens in the femur. By comparison to LAC, we did not observe a statistically significant difference in bacterial burdens in the femurs of mice infected with the sae^C derivative, the Δ*sarA* mutant, or the sae^C/Δ*sarA* mutant (Figure 3). Significantly reduced bacterial burdens were observed in the femurs of mice infected with the Δ*saeRS* mutant. Specifically, no bacteria were recovered from the femurs of 60% of the mice infected with this strain. The number of bacteria recovered from the remaining 40% of these mice ranged from 10^4 to 10^5 cfu per femur. The reasons for this variability are unclear. However, these experiments were done as two independent biological replicates, and most, but not all, of the mice in which no viable bacteria were recovered were included in the first replicate. Nevertheless, these results are consistent with a previous report that also found that bacterial burdens were reduced in a LAC Δ*sae* mutant.[5] Moreover, no viable bacteria were recovered from any of the femurs of mice infected with the Δ*saeRS*/Δ*sarA* double mutant (Figure 3). This suggests that *sarA*, which had not been previously examined in this regard, also contributes to the ability of *S. aureus* to persist in the bone as defined by the 14-day postinfection period we employed and that concomitant mutation of *saeRS* and *sarA* has an additive effect in this regard. Taken together with the μCT data, our results indicate that *saeRS* and *sarA* contribute to the pathogenesis of OM to a comparable degree.

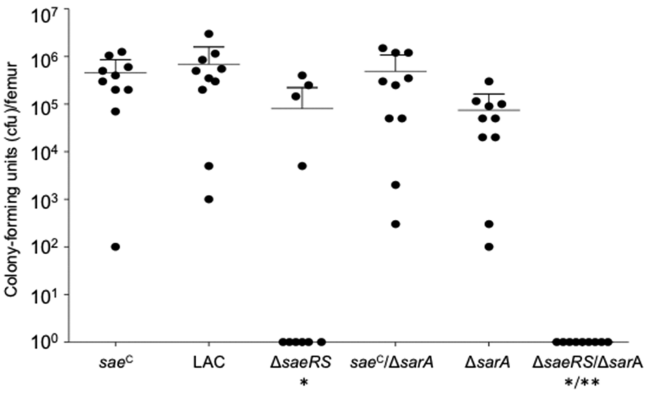

Figure 3. Bacterial burdens in the bone as a function of *saeRS* and *sarA*. Femurs were harvested from mice infected with each of the indicated strains 14 days after infection. Femurs were flash frozen, pulverized, and sonicated before removing tissue debris by low speed centrifugation. Supernatants were then serially diluted and plated on TSA to determine the number of viable bacteria per femur. Single asterisk (*) indicates a significant difference relative to LAC. Double asterisks (**) indicates a statistical significance relative to the Δ*saeRS* mutant.

Correlations between Virulence, Protease Production, and Protein Abundance. Mutation of *saeRS* or *sarA* has been shown to result in the increased production of extracellular proteases, and this has been correlated with reduced accumulation of specific virulence factors and reduced virulence.[6−8] We confirmed that mutation of *saeRS* or *sarA* results in increased protease activity and that mutation of *sarA* has a much greater impact in this regard than mutation of *saeRS* (Figure 4). The impact of mutating *saeRS* and *sarA* on protease production was additive in that a statistically significant difference was observed between the *sarA* and *saeRS*/*sarA* mutants. Conversely, protease production was reduced in the Δsae^C/*sarA* mutant relative to the isogenic Δ*sarA* mutant. Although the difference in virulence between the Δsae^C/*sarA* and *sarA* mutants did not reach statistical significance (Figure 2), this is consistent with the trends we observed in our OM comparisons, and in this case the

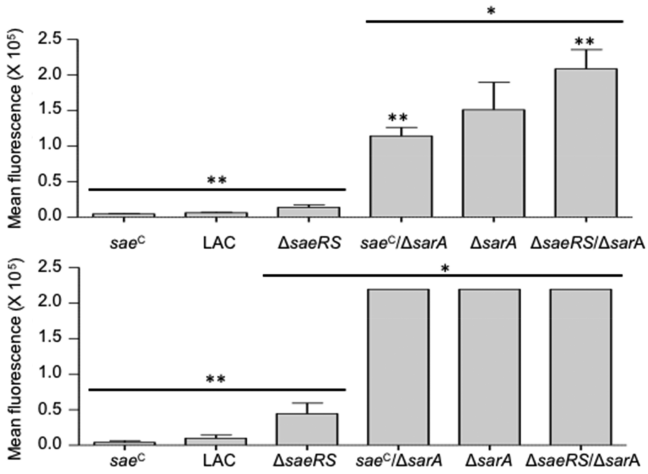

Figure 4. Impact of *saeRS* and *sarA* on protease activity. Overall protease activity was determined in conditioned medium (CM) from stationary phase cultures of LAC, its *sarA* mutant (Δ*sarA*), and isogenic derivatives of each in which *saeRS* was either constitutively expressed (sae^C) or mutated (Δ*saeRS*). Protease activity was determined using a FRET based assay (EnzChek Gelatinase/Collagenase Assay Kit, Molecular Probes) after incubation for 2 h (top) or 16 h (bottom). Statistical analysis was done by one-way ANOVA with Dunnett's correction. A single asterisk (*) indicates a significant difference relative to LAC. Double asterisks (**) indicate statistical significance relative to the *sarA* mutant.

DOI: 10.1021/acsinfecdis.9b00291
ACS Infect. Dis. 2020, 6, 237−249

difference between the Δ*sae*^{C}/*sarA* and Δ*sarA* mutants was statistically significant (Figure 4).

The relative levels of protease production were inversely correlated with the accumulation of high-molecular weight proteins as assessed by SDS-PAGE analysis of conditioned medium (CM) from stationary phase cultures of each of these strains. CM samples from stationary phase cultures were chosen because protease production is highest in this growth phase. We also believe that stationary phase cultures are most likely to be representative of in vivo growth conditions. Evidence to support this hypothesis comes from the observation that protease-deficient mutants have been shown to be hypervirulent in vivo in diverse animal models of infection.[9,10] The abundance of high molecular weight proteins was dramatically reduced in CM from the Δ*sarA* mutant, with a corresponding increase in the abundance of lower molecular weight proteins (Figure S1). This was true irrespective of the functional status of *saeRS*, although overall protein profiles of CM from the *sae*^{C}/Δ*sarA* and Δ*saeRS*/Δ*sarA* mutants did differ from each other and from that observed in the isogenic Δ*sarA* mutant. This is consistent with the relative level of protease production in these strains, and it provides an additional indication that the functional status of *saeRS* has an impact on the phenotype of a LAC Δ*sarA* mutant. In contrast, the abundance of many proteins, including high molecular weight proteins, was reduced in CM from a Δ*saeRS* mutant, but the overall distribution of these proteins was largely unaffected (Figure S1). These observations are consistent with the hypothesis that mutation of *saeRS* impacts the abundance of *S. aureus* exoproteins primarily at the level of their production, while mutation of *sarA* does so primarily at the level of their accumulation owing to protease-mediated degradation.

To further examine this hypothesis, we carried out gel-based proteomic studies employing a novel mass-based approach that allowed us to focus specifically on spectral counts derived from full-length proteins to the exclusion of spectral counts derived from degradation products of those proteins.[11] On the basis of triplicate samples, and irrespective of the abundance of each protein, we identified an average of 1090 full-length proteins in CM from LAC and 1007 in CM from its *sae*^{C} derivative (Figure 6). An average of 763 (≥70%) of these were detectable in CM from the Δ*saeRS* mutant. In contrast, an average of 145 and 160 full-length proteins (≤15.9%) were detected in CM from the isogenic Δ*sarA* and Δ*saeRS*/Δ*sarA* mutants, respectively. This number was more than doubled to an average of 349 in the *sae*^{C}/Δ*sarA* mutant (Figure 5), likely owing to increased protein production associated with the *sae*^{C} allele.

To assess the abundance of individual proteins, we carried out an analysis based on total spectral counts derived from full-length proteins rather than the total number of detectable proteins. The number of spectral counts was highest in the *sae*^{C} derivative (average = 21 356), slightly lower in LAC (18 709) and decreased progressively through the Δ*saeRS* (8485), *sae*^{C}/Δ*sarA* (5478), Δ*sarA* (3223), and Δ*saeRS*/Δ*sarA* mutants (1746) (Figure 5). The fact that ≥70% of full-length proteins that were detectable in LAC and its *sae*^{C} derivative were also detectable in the Δ*saeRS* mutant, while this proportion was reduced to ≤45% when comparisons were made based on total spectral counts, is consistent with the hypothesis that the primary mechanism by which *saeRS* impacts exoprotein accumulation is at the level of production. Similarly, the fact

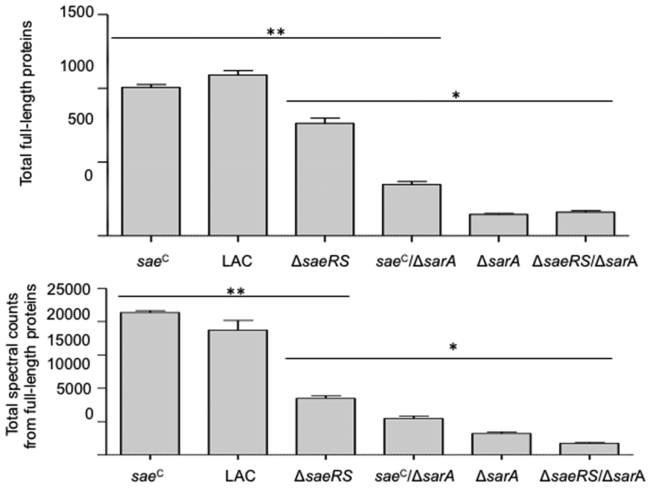

Figure 5. Impact of *sarA* and *saeRS* on relative abundance of full-length proteins. CM from LAC and five derivatives that differ with respect to the functional status of *saeRS* and *sarA* was analyzed in triplicate using a novel mass-based proteomics approach that allows us to focus on quantifying only full-length functional proteins.[11] The top panel illustrates the average number of full-length proteins identified in CM from each strain irrespective of the amount of each protein. The bottom panel illustrates the average number of spectral counts obtained from full-length proteins in CM from each strain. Statistical analysis was done by one-way ANOVA with Dunnett's correction. A single asterisk (*) indicates a significant difference relative to LAC. Double asterisks (**) indicate statistical significance relative to the *sarA* mutant.

that the decrease observed with the Δ*sarA* mutant was comparable whether assessed by total proteins (≤14%) or spectral counts (≤17%) is consistent with the hypothesis that the impact of mutating *sarA* occurs primarily at the level of protease-mediated degradation. However, irrespective of the mechanism responsible, the association between relative virulence (Figure 2) and the number of spectral counts derived from full-length proteins (Figure 5) suggests that defining correlations among these strains between relative virulence and protein abundance as defined based on spectral counts derived from full-length proteins has the potential to identify *S. aureus* virulence factors that are potentially important in the pathogenesis of OM.

To this end, we explored two different methods of data analysis to identify proteins that were increased in abundance in LAC and its *sae*^{C} by comparison to all four of the attenuated strains (Δ*saeRS*, *saeRS*^{C}/Δ*sarA*, Δ*sarA*, Δ*saeRS*/Δ*sarA*). In the first approach, we did individual pairwise comparisons (*t* test) between each of the two most virulent strains and each of the four attenuated strains. Comparisons were made on the basis of statistical significance ($p \leq 0.05$) using a $\log_2$ fold-change (FC) cutoff of ≥2, which corresponds to an absolute FC ≥ 4. The list of proteins meeting these criteria in each pairwise comparison was then compared, using Venny 2.1,[12] to identify proteins that were increased in both virulent strains by comparison to all four attenuated mutants. This resulted in the identification of a common set of 114 proteins (Figure 6 and Table S1).

To prioritize among these 114 proteins, we increased the stringency to a $\log_2$ FC ≥ 5, which corresponds to an absolute FC ≥ 32. This narrowed the list of high priority targets that differed between virulent and attenuated strains from 114 to 10. To validate these results, we also analyzed the entire

DOI: 10.1021/acsinfecdis.9b00291
ACS Infect. Dis. 2020, 6, 237−249

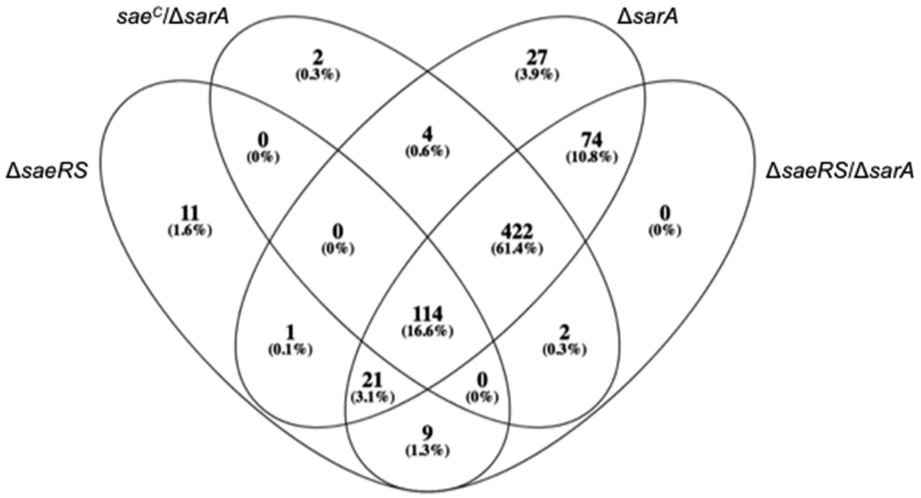

Figure 6. Venn diagram indicating overlap between proteins present in conditioned medium from LAC and its *saeRS* and *sarA* mutants. Conditioned medium (CM) from three independent stationary phase cultures of each strain were resolved by SDS-PAGE and stained with Coomassie Blue (Figure S1). The number of proteins identified as significantly differing ($p \leq 0.05$; $\log_2$ FC ≥ 2) between both of the virulent strains (*sae*^{C} and LAC) compared to each attenuated strain are shown.

proteome data set using the edgeR generalized linear model quasi-likelihood (glmQLT) method.[13,14] This statistical analysis allowed us to compare spectral counts obtained from full-length proteins present in CM from the virulent (LAC and its *sae*^{C} derivative) vs attenuated (*sae*^{C} and LAC vs Δ*saeRS*, *sae*^{C}/Δ*sarA*, Δ*sarA*, Δ*saeRS*/Δ*sarA*). Using this approach, we identified 333 proteins that were significantly increased ($p \leq 0.05$; $\log_2$ FC ≥ 2) in both virulent strains by comparison to all four attenuated strains (Figure 7 and Table S2). To further prioritize among these, we then selected those proteins exhibiting a $\log_2$ FC ≥ 5. Using this approach, 11 proteins were identified that differed in abundance between virulent and attenuated strains.

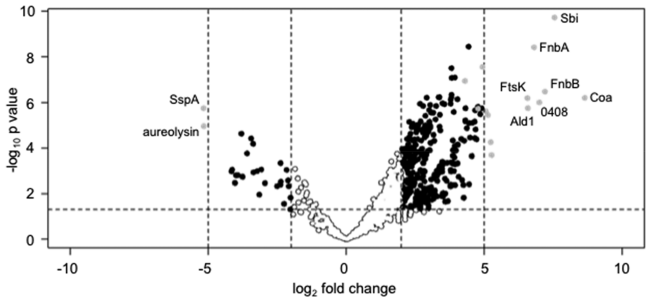

Figure 7. Differential protein accumulation in virulent versus attenuated strains. Volcano plot showing the $\log_2$ fold change (*x*-axis) and $-\log_{10}$ FDR-adjusted *p*-value (*y*-axis) of each protein identified in each strain. Inner vertical lines indicate a $\log_2$ fold change of 2.0. Outer vertical lines indicate a $\log_2$ fold change of 5.0. Proteins that were not found to differ significantly (as defined by an FDR corrected *p*-value ≥0.05 and a fold change ≤2) between virulent and attenuated strains using the quasi-likelihood analysis method are shown as open circles. Proteins in which the abundance was statistically significant ($p \leq 0.05$) and the $\log_2$ fold change ≥2.0 but ≤5.0 as defined by both data analysis methods are shown in black. Proteins in which the $\log_2$ fold change was ≥5.0 as defined by at least one data analysis method are shown in gray. The 7 proteins identified as present in significantly increased amounts in both virulent strains by comparison to all four attenuated strains by both analysis methods are labeled in the upper right quadrant.

The list of proteins prioritized with each analysis method were similar but not identical. Thus, using both analysis methods we identified a total of 14 proteins that differed in abundance by a $\log_2$ FC ≥ 5 in both virulent strains vs all four attenuated strains (Table 1). Of these, 3 were identified using the pairwise analysis method but not the quasi-likelihood GLM method (Table 1). Similarly, 4 were identified using the quasi-likelihood GLM method but not the pairwise analysis method. The other 7 proteins were identified using both data analysis methods (Table 1, Figure 7). These 7 proteins were the fibronectin-binding proteins FnbA and FnbB, Sbi, staphylocoagulase, an FtsK/SpoIII family protein, alanine dehydrogenase 1, and an uncharacterized putative surface protein encoded by SAUSA300_0408. All 7 of these were also identified in our previous study focusing solely on identifying proteins that are present in reduced amounts in a LAC *sarA* mutant owing to protease-mediated degradation,[11] an observation that we believe further validates our experimental approach. It is also interesting to note that the only two proteins found to be present at a level $\log_2$ FC ≥ 5 in all four attenuated strains vs both of the more virulent strains were the extracellular proteases aureolysin and SspA (Figure 7).

Investigating the Role of Staphylocoagulase. As a first step toward ultimately examining the hypothesis that the specific proteins identified in our studies play a role in the pathogenesis of OM, we began the process of generating mutations in the genes encoding these proteins. We initially employed transduction from existing mutants in the Nebraska Transposon Mutant Library (NTML),[15] and among the first of our successful transductions was the mutation in the gene encoding staphylocoagulase (*coa*). We chose to move forward with these mutants based on previous reports suggesting that coagulase plays an important role in immune evasion, biofilm formation[16] and osteoblast physiology.[17] We confirmed that all 7 LAC Δ*coa* mutants generated by transduction from the NTML *coa* mutant exhibited a reduced capacity to form a biofilm by comparison to LAC, albeit to a lesser extent than was observed in the isogenic *sarA* mutant (Figure 8). We also assessed the relative virulence of one of these Δ*coa* mutants in our OM model, and while trends were evident with respect to a reduction in both new bone formation and cortical bone

DOI: 10.1021/acsinfecdis.9b00291
ACS Infect. Dis. 2020, 6, 237−249

Table 1. Proteins Selected as Priority Targets for Further Studies

protein	gene	accession number	localization	molecular weight (kDa)	method
Immunoglobulin-binding protein sbi	*sbi*	SBI_STAA3	unknown	50	both
Staphylocoagulase	*coa*	A0A0H2XHP9_STAA3	extracellular	69	both
Fibronectin binding protein B	*fnbB*	A0A0H2XKG3_STAA3	cell wall	104	both
Alanine dehydrogenase 1	*ald1*	DHA1_STAA3	cytoplasmic	40	both
FtsK/SpolllE family protein	SAUSA300_1687	A0A0H2XK12_STAA3	membrane	145	both
Fibronectin-binding protein A	*fnbA*	FNBA_STAA3	cell wall	112	both
Putative surface protein	SAUSA300_0408	A0A0H2XJZ9_STAA3	unknown	57	both
Uncharacterized leukocidin-like protein 2	SAUSA300_1975	LUKL2_STAA3	extracellular	40	pairwise
Uncharacterized leukocidin-like protein 1	SAUSA300_1974	LUKL1_STAA3	extracellular	39	pairwise
Putative staphylocoagulase	SAUSA300_0773	A0A0H2XEN7_STAA3	extracellular	59	pairwise
Transcriptional regulatory protein WalR	*walR*	WALR_STAA3	cytoplasmic	27	GLM
Uncharacterized protein	SAUSA300_0198	A0A0H2XFU2_STAA3	unknown	36	GLM
Serine protease HtrA-like	SAUSA300_0923	HTRAL_STAA3	unknown	86	GLM
Protein RecA	*recA*	A0A0H2XFW9_STAA3	cytoplasmic	35	GLM

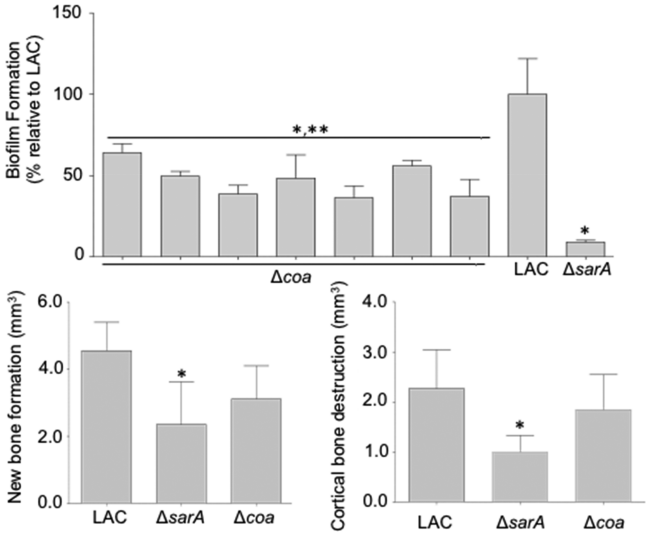

Figure 8. Impact of staphylocoagulase on biofilm formation and osteomyelitis. The top panel illustrates the relative levels of biofilm formation in LAC, its isogenic sarA mutant, and each of 7 independently generated LAC *coa* mutants. Assays were performed in 3 replicates and the average observed with LAC set to 100%. All other results are shown relative to this value. The bottom panel illustrates quantitative assessment of reactive bone formation (left) and cortical bone destruction (right) in Δ*sarA* and Δ*coa* mutants relative to the LAC parent strain. Statistical analysis was done by one-way ANOVA with Dunnett's correction. A single asterisk (*) indicates a significant difference relative to LAC. Double asterisks (**) indicate statistical significance relative to the Δ*sarA* mutant.

destruction, neither of these differences were found to be statistically significant by comparison to LAC (Figure 8).

Investigating Potential Mechanisms of Attenuation Associated with Mutation of *saeRS* and/or *sarA*. The pathogenesis of OM is complex and incompletely understood, but two phenotypes that have been implicated as important contributing factors are biofilm formation and cytotoxicity for osteoblast and/or osteoclasts.[6,9,18−20] These are difficult phenotypes to assess directly in vivo, but they can be readily assessed in vitro. Thus, we examined each of these to determine whether the impact of *saeRS* and *sarA* on these phenotypes could be correlated with relative virulence. As previously demonstrated,[6,7] we found that mutation of *sarA* limited biofilm formation to a much greater extent than mutation of *saeRS*, and this was true irrespective of the functional status of *saeRS* (Figure 9). However, biofilm

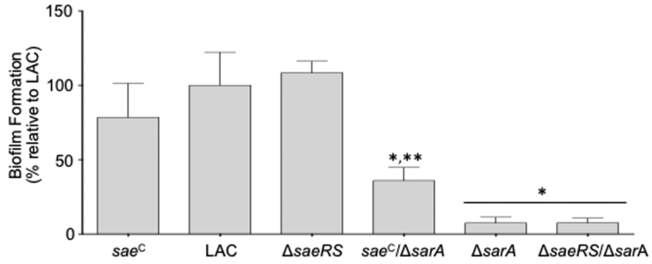

Figure 9. Impact of the functional status of *saeRS* and *sarA* on biofilm formation. Biofilm formation was assessed in each of the indicated strains. Assays were performed in 6 replicates and the average observed with LAC set to 100%. All other results, including each of the 6 individual LAC replicates, are shown relative to this value. Statistical analysis was done by one-way ANOVA with Dunnett's correction. A single asterisk (*) indicates a significant difference relative to LAC. Double asterisks (**) indicate statistical significance relative to the Δ*sarA* and Δ*saeRS*/Δ*sarA* mutants.

formation was increased to a statistically significant extent in the *sae*^{C}/Δ*sarA* mutant relative to the Δ*sarA* and Δ*saeRS*/Δ*sarA* mutants. Similar trends were observed in the context of osteoblast and osteoclast cytotoxicity. Specifically, CM from stationary phase cultures of LAC, its *sae*^{C} derivative, and its Δ*saeRS* mutant were comparably cytotoxic for both cell types, while mutation of *sarA* largely eliminated this cytotoxicity (Figure 10).

A primary reason we carried out these in vitro studies was to determine whether any of these phenotypes could be definitively correlated with differences in virulence we observed in our OM model. If so, this would greatly facilitate the ability to examine a large number of potential targets prior to proceeding to in vivo analysis. However, while biofilm formation and cytotoxicity were significantly reduced in 3 of the 4 attenuated strains, neither was significantly reduced in the Δ*saeRS* mutant. One possible explanation for this is that the magnitude of the impact of mutating *sarA* on protease production as assessed under in vitro conditions is sufficient to be apparent in the context of biofilm formation and cytotoxicity, while the impact of mutating *saeRS* on protease production is not. However, this does not preclude the

DOI: 10.1021/acsinfecdis.9b00291
ACS Infect. Dis. 2020, 6, 237−249

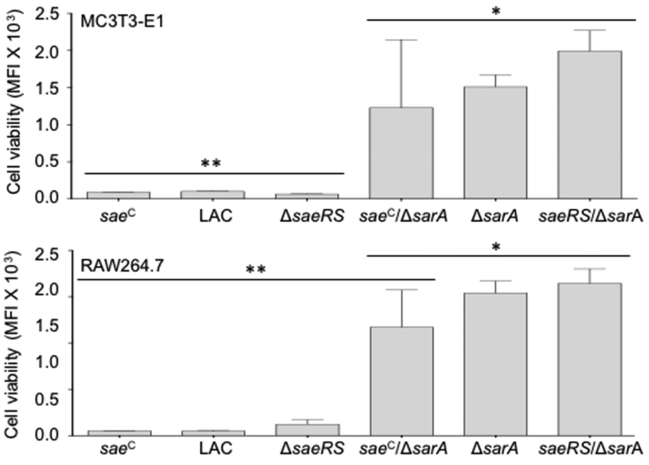

Figure 10. Impact of the functional status of *saeRS* and *sarA* on osteoblast and osteoclast cytotoxicity. Conditioned medium (CM) from stationary phase cultures of the indicated strains were added to monolayers of osteoblast (MC3T3-E1) or osteoclast-like cell lines (RAW264.7) and incubated at 37 °C for 24 h. Cell viability was then determined using a Live/Dead assay kit (Molecular Probes) in which mean fluorescence intensity (MFI) is an indication of cell viability. Statistical analysis was done by one-way ANOVA with Dunnett's correction. A single asterisk (*) indicates a significant difference relative to LAC. Double asterisks (**) indicate statistical significance relative to the Δ*sarA* and Δ*saeRS*/Δ*sarA* mutants.

possibility that mutation of *saeRS* has a greater impact in vivo in the specific microenvironment of bone.

The alternative explanation is that the mechanism by which mutation of *saeRS* attenuates virulence differs by comparison to the mechanism by which mutation of *sarA* attenuates virulence. On the basis of this possibility, we extended our analysis to identify proteins that were present in increased amounts in a LAC Δ*sarA* mutant relative to a Δ*saeRS* mutant and vice versa. Relatively few proteins were present in increased amounts in a Δ*sarA* mutant by comparison to a Δ*saeRS* mutant, but among these were all six of the *spl*-encoded proteases (Figure 11). This is consistent with our

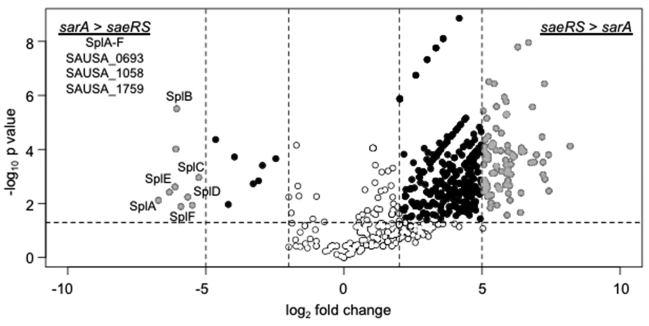

Figure 11. Differential protein accumulation in Δ*saeRS* and Δ*sarA* mutants. Volcano plot showing the $\log_2$ fold change (*x*-axis) and $-\log_{10}$ FDR-adjusted *p*-value (*y*-axis) of each protein identified in each strain. Inner vertical lines indicate a $\log_2$ fold change of 2.0. Outer vertical lines indicate a $\log_2$ fold change of 5.0. Proteins that were not found to differ significantly between the Δ*saeRS* and Δ*sarA* mutants as defined by an FDR corrected *p*-value ≥0.05 and a fold change ≤2 are shown as open circles. Proteins in which the abundance was statistically significant ($p \leq 0.05$) and the $\log_2$ fold change ≥2.0 but ≤5.0 are shown in black. Proteins in which the $\log_2$ fold change was ≥5.0 are shown in gray.

previous reports demonstrating that these proteases are present in reduced amounts in a Δ*saeRS* mutant but increased amounts in an isogenic Δ*sarA* mutant.[7] In contrast, we identified 91 proteins that were present in an increased amount in a Δ*saeRS* mutant by comparison to a Δ*sarA* mutant (Figure 11, Table S3).

Of these, 36 were present in equivalent amounts in CM from the Δ*saeRS* mutant and LAC, thus suggesting that Spl-mediated degradation may be a limiting factor in the accumulation of these proteins in a Δ*sarA* mutant. This also suggests that these proteases, or specific targets of these proteases that are present in decreased amounts in CM from a Δ*sarA* mutant, may contribute to biofilm formation and/or cytotoxicity for osteoblasts and osteoclasts as assessed under in vitro conditions. The remaining 55 proteins were present in decreased amounts in the Δ*saeRS* mutant relative to LAC and its *sae*^{C} derivative. This leaves open the possibility that they contribute to the attenuation of both the Δ*saeRS* and Δ*sarA* mutants in our murine OM model, but are unlikely to contribute to the attenuation of the Δ*saeRS* mutant and not the Δ*sarA* mutant.

Finally, to further examine the hypothesis that mutation of *saeRS* limits virulence in our OM model owing primarily to its impact on protein production, while *sarA* does so owing primary to its impact on protease production and the degradation of *S. aureus* proteins, we generated derivatives of LAC and each of these mutants with a limited capacity to produce extracellular proteases. Specifically, protease-deficient derivatives of LAC and its *sarA* mutant were unable to produce aureolysin, ScpA, SspA, SspB, or any of the *spl*-encoded proteases, while the *saeRS* mutant retained the capacity to produce the *spl*-encoded proteases. However, as discussed above, mutation of *saeRS* does not result in the increased production of these proteases. Eliminating protease production restored biofilm formation and cytotoxicity in the Δ*sarA* mutant, but had little impact in the Δ*saeRS* mutant (Figure 12). This was also true in a LAC Δ*saeRS*/Δ*sarA* mutant. Moreover, as evidenced by visual assessment of μCT images, eliminating protease production restored virulence to a greater extent in the Δ*sarA* mutant than in the Δ*saeRS* mutant, and enhanced the virulence of LAC itself (Figure 13). In fact, the increased virulence observed in the protease-deficient derivatives of LAC and its Δ*sarA* mutant resulted in broken bones to an extent that precluded accurate quantitative analysis of these μCT images.

DISCUSSION

Osteomyelitis is a relatively infrequent form of *S. aureus* infection, but it is one that presents a unique clinical problem that demands an equally unique, multidisciplinary clinical approach.[18] This also applies to infections associated with indwelling orthopedic devices, and in this respect, it is important to recognize that the number of such infections is predicted to increase dramatically in the immediate future. Indeed, it has been estimated that the number of periprosthetic joint infections associated with total hip and knee arthroplasty in the United States will surpass 60 000 by 2020 at an annual cost that will exceed $1.62 billion.[19] This makes it imperative to develop prophylactic and therapeutic strategies that can be used to combat these infections either alone or as a means of enhancing the efficacy of conventional antibiotic therapy.

The studies we report are based on the scientific premise that a key component required for the development of such

DOI: 10.1021/acsinfecdis.9b00291
ACS Infect. Dis. 2020, 6, 237−249

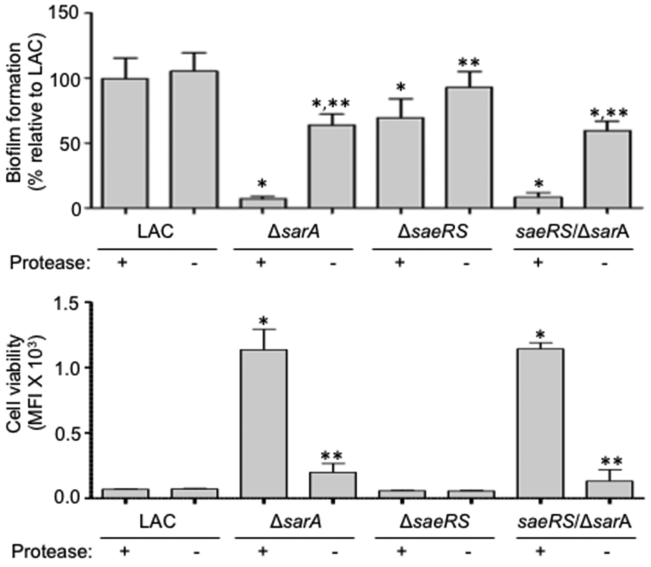

Figure 12. Impact of protease production in Δ*sarA* and Δ*saeRS* mutants in vitro. Biofilm formation (top) and osteoblast cytotoxicity (bottom) were assessed in each of the indicated strains (+) and their protease-deficient derivatives (−). Biofilm assays were performed in 6 replicates and the average observed with LAC set to 100%. All other results, including each of the 6 individual LAC replicates, are shown relative to this value. Cell viability was determined using a Live/Dead assay kit (Molecular Probes) in which mean fluorescence intensity (MFI) is an indication of cell viability. Statistical analysis was done by one-way ANOVA with Dunnett's correction. A single asterisk (*) indicates a significant difference relative to LAC. Double asterisks (**) indicate statistical significance relative to the Δ*sarA* and Δ*saeRS*/Δ*sarA* mutants.

strategies is a clear understanding of the pathogenesis of orthopedic infections that takes into consideration the specific microenvironment of bone. In this respect it is important to note that *S. aureus* is overwhelmingly the primary clinical concern based on both the frequency and severity of the infections caused by this bacterial pathogen.[18,20] It has been demonstrated that expression of *sarA* and *saeRS* is increased during the acute and chronic phases of osteomyelitis,[21,22] and previous reports have demonstrated that mutation of *saeRS* or *sarA* attenuates virulence in a murine model of postsurgical OM.[4,5] This accounts for our experimental focus on these regulatory loci in this report.

In addition, the attenuation of a LAC Δ*saeRS* mutant has been correlated with the increased production of extracellular proteases, specifically aureolysin, and the resulting decrease in the accumulation of phenol-soluble modulins (PSMs), although this could not fully explain the attenuation of a LAC Δ*saeRS* mutant.[4,5] As demonstrated in previous reports,[7,23] and confirmed in the studies reported here, mutation of *sarA* results in a much greater increase in protease production than mutation of *saeRS*. This suggests that mutation of *sarA* would attenuate virulence in OM even by comparison to a Δ*saeRS* mutant.

To address this, we took advantage of our previous studies demonstrating that mutation of *saeRS* or *sarA* attenuates virulence to a comparable degree in a murine bacteremia model[6] to define the relative virulence of LAC and five isogenic derivatives that differ with respect to the functional status of *saeRS* and *sarA* in a murine model of postsurgical OM. The results demonstrated that mutation of *saeRS* or *sarA* also attenuates virulence in this model to a comparable degree (Figure 2). The attenuation observed with the LAC Δ*sarA* mutant was reversed to a limited extent in the sae^{C}/*sarA* mutant, but the difference was not statistically significant in the

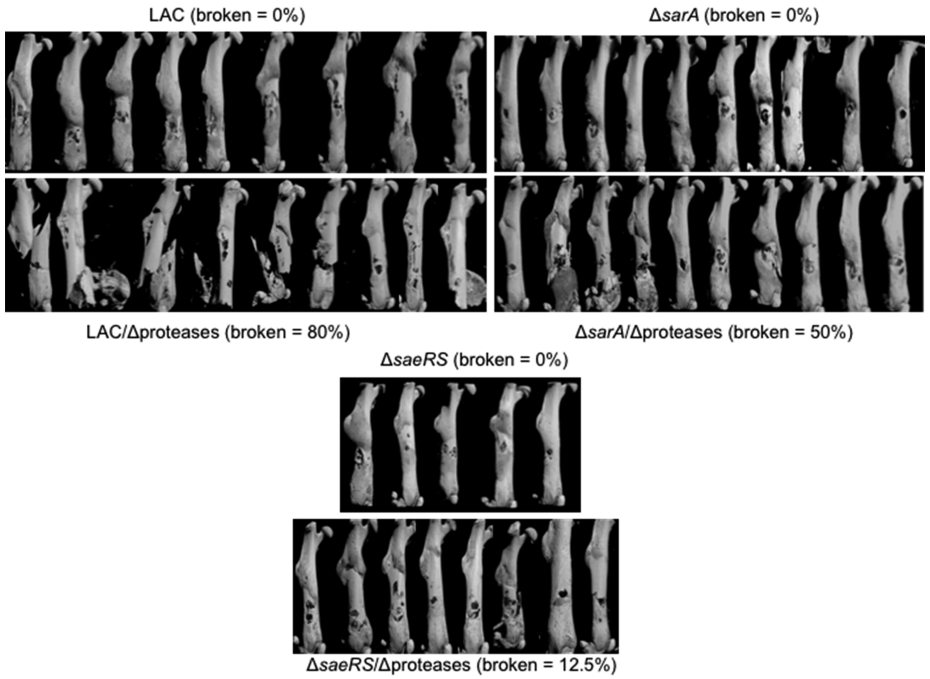

Figure 13. Impact of protease production in Δ*sarA* and Δ*saeRS* mutants in vivo. A murine model of post-traumatic osteomyelitis was used to assess the relative virulence of LAC, its Δ*sarA* and Δ*sae* mutants, and protease-deficient derivatives of each strain (Δprotease). All images from all mice in each experimental group are shown for comparison along with the percentage of femurs from all animals within each group in which the femur was broken.

DOI: 10.1021/acsinfecdis.9b00291
ACS Infect. Dis. 2020, 6, 237−249

context of either μCT analysis or bacteriological burdens in the femur. Mutation of *saeRS* did have a greater impact than mutation of *sarA* on bacterial burdens in the femur (Figure 3). However, mutation of *saeRS* and *sarA* had an additive effect in this regard, thus suggesting that both loci contribute to the ability of *S. aureus* to colonize and persist in the bone.

Although mutation of *saeRS* and mutation of *sarA* had a comparable impact on virulence but not on protease production, the accumulation of any protein is a function of its production vs its degradation. Indeed, we previously proposed that the primary impact of mutating *saeRS* on the virulence of *S. aureus* is mediated at the level of virulence factor production while that of mutating *sarA* is mediated at the level of the protease-mediated degradation of these virulence factors. The results we report here provide further support for this hypothesis. Specifically, mutation of *saeRS* resulted in a protein profile that included the majority of proteins present in LAC and its sae^C derivative, albeit in reduced amounts, while the protein profile of the isogenic Δ*sarA* mutant was characterized by a lack of high-molecular weight proteins (Figure S1). However, differences in the relative impact of extracellular proteases in a Δ*sarA* mutant vs a Δ*saeRS* mutant do not preclude the possibility that mutation of these loci impacts the accumulation of an overlapping set of proteins that are relevant in the pathogenesis of OM. Indeed, there are reports describing transcriptional changes associated with OM,[21,22] but the results we report suggest that a better approach would be to consider virulence differences in the context of protein accumulation rather than transcriptional changes alone.

To address this, we utilized a novel mass-based proteomic approach recently developed and validated in our laboratories that allows us to focus on spectral counts derived from full-length proteins to the exclusion those derived from degradation products of those proteins.[11] The results confirmed that the accumulation of full-length proteins is significantly reduced in all four of the strains found to be attenuated in our murine OM model compared to the virulent strains LAC and its sae^C derivative (Figure 5). Using a stringent cutoff of a $\log_2$ fold-change of ≥5.0 (absolute fold-change ≥32) and each of two data analysis methods, we identified 14 proteins that were more abundant in both virulent strains by comparison to all four attenuated strains (Table 1, Figure 7). This suggests to us that these proteins are of potential interest in the pathogenesis of OM. However, we are not suggesting that these 14 proteins are the only proteins of potential interest. For instance, staphylococcal protein A (Spa) was not included among the priority list of 14 proteins, and it has been implicated in the pathogenesis of OM.[24−28] Moreover, the abundance of Spa was reduced to a statistically significant extent in all four attenuated strains (Figure S2) and did not meet the highly stringent standards we chose to employ only because of its relatively high abundance in the Δ*saeRS* mutant. Thus, it could be argued that these standards are too stringent. However, we believe that the methods we employed are appropriate in that they increase the likelihood of identifying high-priority targets that warrant further examination. In fact, we used two different data analysis methods to further increase the stringency of our approach, and this reduced this group of high-priority targets from 14 to 7 based on the fact that they were identified using both methods.

Included among these 7 proteins were the fibronectin-binding proteins FnbA and FnbB. This is potentially relevant in that these proteins have been implicated in biofilm formation, which is a key component of many types of *S. aureus* infection including OM[29−31] An FtsK/SpoIII family protein was also identified using both analysis methods. The other two proteins included in the list of 7 that were identified by both analysis methods were an uncharacterized putative surface protein (SAUSA300_0408), which was also identified in a previous report focusing solely on the role of *saeRS* OM,[5] and alanine dehydrogenase 1. The latter is a cytoplasmic protein, but this does not preclude the possibility that it may act as a "moonlighting" virulence factor, particularly given that other dehydrogenases have been reported to moonlight on the cell surface promoting adhesion to extracellular matrix proteins.

Also included were the immunoglobulin binding protein Sbi and staphylocoagulase, both of which have been implicated as important components of immune evasion.[32−38] Other reports have concluded that coagulase production contributes to biofilm formation[16] and, at least as assessed under in vitro conditions, osteoblast physiology and bone destruction.[17] As further validation of our experimental approach, we demonstrated that LAC Δ*coa* mutants have a reduced capacity to form a biofilm and exhibit a modest reduction in virulence in our OM model (Figure 8). The fact that mutation of *coa* had less impact on biofilm formation and virulence in our OM model than mutation of *sarA* is not unexpected given that mutation of *sarA* limits the accumulation of many *S. aureus* proteins of potential relevance. This was also true with respect to osteoblast and osteoclast cytotoxicity, which was significantly reduced in a *sarA* mutant but not in a *coa* mutant (Figure S3). Nevertheless, these results suggest that coagulase does play a role in OM as previously suggested.[16,17] They also suggest that the impact of mutating *saeRS* or *sarA* on the pathogenesis of OM is likely to be multifactorial.

From a mechanistic point of view, there are two considerations that we tried to take into account. The first is whether we could identify any in vitro phenotypes that could be directly correlated with virulence. This was based on the hope such phenotypes could be used to further prioritize *S. aureus* proteins of potential interest before pursuing in vivo studies. However, while there were clear correlations, none of the in vitro phenotypes we examined could be definitively correlated with relative virulence. This includes protease production, biofilm formation and cytotoxicity for osteoblasts and osteoclasts. The second consideration is the manner by which mutation of *saeRS* and *sarA* limits virulence in our OM model, and in this respect we believe the results we report provide further support for the hypothesis that mutation of *saeRS* does so by limiting the production of important virulence factors, while *sarA* does so by limiting their accumulation owing to the increased production of extracellular proteases. Thus, in effect mutation of *saeRS* vs *sarA* represent two distinct means to the same end, that being reduced virulence in the specific clinical context of osteomyelitis.

This is consistent with the observation that eliminating protease production restored virulence in the Δ*sarA* mutant to a greater extent than was observed in the isogenic Δ*saeRS* mutant (Figure 13). In fact, eliminating the production of extracellular proteases in the Δ*sarA* mutant and even in LAC itself enhanced virulence in our OM model to an extent to

DOI: 10.1021/acsinfecdis.9b00291
ACS Infect. Dis. 2020, 6, 237−249

which the proportion fractured bones precluded accurate quantitative μCT analysis (Figure 13). However, protein production vs degradation are not mutually exclusive functions, and this does not mean that increased protease production is irrelevant in a LAC Δ*saeRS* mutant. Rather, it just suggests that the relatively modest impact of mutating *saeRS* on protease production may be phenotypically apparent only because the amount of many *S. aureus* proteins is already limited in the Δ*sae* mutant. Nevertheless, this does not preclude the possibility that mutation of *saeRS* and/or *sarA* results in the reduced accumulation of common *S. aureus* proteins that contribute to the pathogenesis of OM either alone or in combination with each other, and we believe the results of the experiments we report have allowed us to identify and prioritize specific proteins of interest in this regard.

At the same time, it is also possible that the attenuation of LAC Δ*sarA* and Δ*saeRS* mutants can be attributed to the impact of these mutations on different *S. aureus* proteins, and the experimental approach we describe would preclude the identification of such proteins. This possibility prompted us to make proteomic comparisons between the Δ*sarA* and Δ*saeRS* mutants themselves (Figure 11). The results confirmed that the abundance of 91 proteins was elevated in the Δ*saeRS* mutant by comparison to the Δ*sarA* mutant. However, the abundance of the majority of these was still reduced by comparison to LAC itself. The extent to which the abundance of any given protein must be reduced to have a phenotypic impact in vivo is not known, thus leaving open the possibility that the reduced abundance of these proteins contributes to the attenuation of the Δ*saeRS* mutant by comparison to LAC and its *sae*^{C} derivative. However, since these 91 proteins were more abundant in Δ*saeRS* than Δ*sarA* mutants, it seems unlikely they would contribute to the attenuation of the Δ*saeRS* mutant but not the Δ*sarA* mutant.

In contrast, very few proteins were present in increased amounts in the Δ*sarA* mutant by comparison to the Δ*saeRS* mutant. Interestingly, this did include all six of the *spl*-encoded proteases. This is consistent with previous reports demonstrating that the abundance of these proteases is increased in a Δ*sarA* mutant but not in a Δ*saeRS* mutant.[5,9] This suggests that specific targets of these proteases, or the proteases themselves, may contribute to the reduced biofilm formation and cytotoxicity observed with the Δ*sarA* mutant as assessed under in vitro conditions.

Finally, the proteomic approach we described can also be used to identify *S. aureus* proteins that are less likely to be involved in the pathogenesis of OM (Table S4). For instance, LukD, LukF, and LukS were all present in increased amounts in a LAC Δ*sarA* mutant by comparison to the isogenic Δ*saeRS* mutant. The abundance of these proteins in the Δ*saeRS* mutant was comparable to LAC itself. This suggests that these exotoxins are unlikely to contribute to the attenuation of the Δ*sarA* or Δ*saeRS* mutants. With respect to LukF and LukS, this is consistent with the observation that mutation of *sarA* also limits virulence in the methicillin-sensitive strain UAMS-1,[4] which does not encode either of these genes.

CONCLUSION

The results we report demonstrate that mutation of *saeRS* or *sarA* in the USA300 strain LAC attenuates virulence to a comparable degree in a murine model of postsurgical OM to a comparable degree. Our results also support the conclusion that the primary impact of mutating *saeRS* is mediated at the level of protein production, while that of mutating *sarA* is mediated at the level of protease-mediated protein degradation. Irrespective of the underlying mechanism that limits their accumulation, this opens up the possibility of identifying and prioritizing *S. aureus* virulence factors of potential relevance in the specific context of OM based on a correlation between their relative abundance in *S. aureus* strains that are demonstrably different with respect to virulence in this important clinical context. Because mutation of *saeRS* or *sarA* impacts the accumulation of a large number of possible virulence factors, prioritization is a key element of our approach, and in this regard, we purposefully applied a very stringent standard in the analysis of our proteomic comparisons. This accounts for our primary focus on 7 proteins, but it certainly does not preclude the possibility that other proteins not among this primary group are also important. Nevertheless, we believe the results we report clearly indicate that these proteins warrant direct examination as virulence factors of potential relevance in the pathogenesis of OM.

EXPERIMENTAL SECTION

Ethics Statement. All experiments involving animals were reviewed and approved by the Institutional Animal Care and Use Committee of the University of Arkansas for Medical Sciences and performed according to NIH guidelines, the Animal Welfare Act, and United States federal law.

Bacterial Strains and Growth Conditions. The bacterial strains used in this study were previously described.[6,39,40] Briefly, an erythromycin-sensitive derivative of the USA300 strain LAC was used as the parent strain from which the isogenic derivatives *sae*^{C}, Δ*saeRS*, *sae*^{C}/Δ*sarA*, Δ*sarA*, and Δ*saeRS*/Δ*sarA* were generated. The Δ*saeRS*/Δprotease mutant was made by transduction of the *saeRS* mutation into a LAC derivative containing mutations in *sspAB*, *scpA*, and the gene encoding aureolysin (*aur*). These mutations were generated using the pKOR derivative pJB38 for *sspAB* and *scpA* and the pKOR1::*aur* construct for *aur*. The Δ*sarA*/Δprotease mutant was made by transduction of the *sarA* mutation[20] into a LAC derivative unable to produce these same proteases as well as those encoded by the *spl* operon.[40] Strains were maintained at −80 °C in tryptic soy broth (TSB) containing 25% (v/v) glycerol. For each experiment, strains were retrieved from cold storage by plating on tryptic soy agar[41] with appropriate antibiotic selection. Antibiotics used were erythromycin (5 μg/mL), tetracycline (5 μg/mL), kanamycin (50 μg/mL), and neomycin (50 μg/mL).

Murine Model of Osteomyelitis. Induction of OM was done as previously described.[5,6] Briefly, 6−8 week-old C57BL/6 female mice were anesthetized and an incision made in the right hind limb to expose the femur. Using a precision needle, a unicortical defect was created at the midfemur. The intramedullary canal was inoculated via the unicortical defect with 2 μL of a bacterial suspension containing 1×10^6 cells harvested from midexponential phase (OD_{560} = 1.0) cultures. Muscle and skin were sutured, and the infection allowed to proceed for 14 days. After this time, mice were euthanized and the infected femurs harvested for microcomputed tomography (μCT) analysis or quantitation of the bacterial burden.

Microcomputed Tomography (μCT). Image acquisition and analysis were done according to protocols described elsewhere with minor modifications.[4,5] Briefly, imaging was be performed with the Skyscan 1174 X-ray Microtomograph

DOI: 10.1021/acsinfecdis.9b00291
ACS Infect. Dis. 2020, 6, 237−249

(Bruker, Kontich, Belgium) using an isotropic voxel size of 6.7 μm, an X-ray voltage of 50 kV (800 μA) and a 0.25 mm aluminum filter. Reconstruction was carried out using the Skyscan Nrecon software. The reconstructed cross-sectional slices were processed using the Skyscan CT-analyzer software as follows: first, bone tissue was isolated from the soft tissue and background using a global thresholding (low = 85; high = 255). Using the bone-including binarized images a semi-automated protocol was run to delineate regions of interest where the reactive new bone (callus) was isolated from the cortical bone (this protocol is a morphological escalator that separates the reactive bone structures using multiple rounds of opening and closing of gaps using increasing preset diameters for each round). The resulting images were loaded as ROI and corrected by drawing inclusive or exclusive contours on the periosteal surface to keep only and strictly the cortical bone. Using these defined ROI, the volume of cortical bone was calculated, and the amount of cortical bone destruction estimated by subtracting the value obtained from each bone from the average obtained from sham operated bones inoculated with PBS. New bone formation was quantified using the subtractive ROI function on the previously delineated cortical bone-including ROI images and calculating the bone volume included in the newly defined ROI. Statistical analysis of data from each experimental group was done by one-way ANOVA with Dunnett's correction. Separate comparisons were made with all strains relative to LAC or to its Δ*sarA* mutant. A *p*-value ≤0.05 was considered statistically significant.

Bacterial Burdens in the Femur. Bacterial loads in each femur were determined as previously reported.[5] Briefly, femurs were separated from surrounding soft tissue, frozen in liquid nitrogen, and homogenized. Homogenized bones were resuspended in 1 mL PBS. Subsequently, homogenates were sonicated, vortexed, serially diluted and plated on TSB solidified with 1.5% agar. Colony forming units (cfu) were counted and differences between groups of mice assessed using a one-way analysis of variance (ANOVA) model. Briefly, cfu data was logarithmically transformed prior to analysis. For samples with no bacterial counts, a number near 1 was added to each cfu value before the transformation was applied. Contrasts were defined to assess the comparisons of interest. Adjustments for multiple comparisons were made using simultaneous general linear hypothesis testing procedures.[42] Adjusted *p*-values ≤0.05 were considered significant. Analyses were done using R (version 3.4.3, R Foundation for Statistical Computing, Vienna, Austria). Multiple comparison procedures were implemented using the R library multcomp.

Extracellular Protease Activity. Overnight cultures grown in 5.0 mL of TSB without antibiotic selection were standardized relative to each other based on optical density (OD_{560} = 10) and cells removed by centrifugation. Supernatants were then filter sterilized (0.2 μm) to obtain conditioned media (CM). Protease activity in these samples was assessed using the EnzChek Gelatinase/Collagenase Assay Kit (Thermo). Fluorescence was measured after 2 and 16 h of incubation. Statistical analysis was done by one-way ANOVA with Dunnett's correction. Separate comparisons were made with all strains relative to LAC or to its Δ*sarA* mutant. A *p*-value ≤0.05 was considered statistically significant.

Biofilm Formation. These assays were done as previously described.[43] Briefly, overnight cultures grown in biofilm media (TSB supplemented with glucose and sodium chloride) without antibiotic selection were standardized (OD_{540} = 0.05) and inoculated into a microtiter plate where the wells were coated with human plasma proteins beforehand.[6,7,23,41,43,44] Biofilm formation was then assessed after 24 h. Statistical analysis was done by one-way ANOVA with Dunnett's correction. Separate comparisons were made with all strains relative to LAC or to its Δ*sarA* mutant. A *p*-value ≤0.05 was considered statistically significant.

Cytotoxicity Assay. These assays were done according to a previously reported protocol.[4] Briefly, MC3T3-E1 and RAW 264.7 cells were seeded into black 96 well microtiter plates with a clear bottom at densities of 10 000 and 50 000 cells/well, respectively. After 24 h the media was replaced with a 1:1 mixture of cell media and CM standardized as described above (OD_{540} = 10). Plates were incubated for 24 h. Cytotoxicity was determined using the LIVE/DEAD Viability/Cytotoxicity Kit for mammalian cells (Thermo Fisher Scientific). Statistical analysis was done by one-way ANOVA with Dunnett's correction. Separate comparisons were made with all strains relative to LAC or to its Δ*sarA* mutant. A *p*-value ≤0.05 was considered statistically significant.

Exoprotein Profile Analysis. Assessment of the secreted proteome was performed in triplicate as previously described.[11] Briefly, an equal volume of standardized CM from each sample was resolved by one-dimensional SDS-PAGE and visualized by Coomassie-staining. Each gel lane was sliced into 24 equiv bands of 2 mm each. Gel bands were destained, reduced, alkylated, dehydrated, and trypsin digested. Acidified tryptic peptides were separated using reverse phase UPLC. Eluted peptides were ionized by electrospray (2.15 kV) followed by MS/MS analysis using higher-energy collisional dissociation (HCD) on an Orbitrap Fusion Tribrid mass spectrometer (Thermo) in top-speed data-dependent mode. MS/MS data were acquired using the ion trap analyzer and proteins were identified by database search using Mascot (Matrix Science, version 2.5.1) against the USA300 *S. aureus* database (2653 entries, GenBank accession JTJK01000002). A decoy database (based on the reverse of the protein sequences) was used in the search to calculate the FDR for the search algorithm. Scaffold (Proteome Software) was used to verify MS/MS based peptide and protein identifications (FDR < 1%; identified peptides ≥ 2). Total spectral counts for each replicate were exported from Scaffold into Microsoft Excel and R for further analysis.

Data analysis was done as previously described.[11] Briefly, spectral count data collected from wild-type was used to locate the gel band with the maximum spectral count for a given protein. Spectral count observed in this band were added to spectral count observed in the gel bands immediately above and below to obtain total spectral count in a 3-band continuous window corresponding to the overall spectral peak for each full-length protein. A counts matrix for all samples including each of the replicates was generated based on this 3-band window. For the first analysis method the spectral count for each identified protein in each of the virulent strains was compared to the spectral count in each of the attenuated strains using two tailed *t* tests. Proteins with $p > 0.05$ were filtered out from each comparison. For the proteins with $p \leq 0.05$, the fold change was determined, first with a cutoff of $\log_2$ FC ≥ 2 and, then with a cutoff of $\log_2$ FC ≥ 5. The resulting lists of the proteins meeting these criteria in each pairwise comparison were then compared using Venny (version 2.1) to identify commonalities and differences

DOI: 10.1021/acsinfecdis.9b00291
ACS Infect. Dis. 2020, 6, 237−249

between each set of comparisons. For the second analysis method, the spectral counts were imported into R for statistical analysis using the EdgeR Bioconductor package.[13,14] The spectral counts were normalized using Trimmed Mean of M-values (TMM) prior to performing the generalized linear model quasi-likelihood ratio test. Data visualization images were generated using R studio.

Mutation of *coa*. The mutated *coa* gene was moved to LAC via transduction from a donor strain obtained from the Nebraska Transposon Mutant Library (NTML)[15] through BEI Resources (Manassas, VA; http://www.beiresources.org). The isogenic LAC Δ*coa* mutants were validated with a PCR validated by PCR using primers specific for the *coa* gene (5′ GCTAGGCGCATTAGCAGTTG and 3′ TCGTAACTCT-TTCGCGTGCT). These oligos bind to sites flanking the transposon insertion site. The genetic background of these mutants was also verified with a PCR specific for the small cryptic plasmid present in LAC and absent in the plasmid curated LAC derivative strain, JE2, in which the NTML was generated (data not shown). The primers used for this PCR were 5′ CCGAGGCTCAACGTCAATAA, 3′ GCAGT-TGGTGGGAACTACAA.

■ ASSOCIATED CONTENT

Supporting Information

The Supporting Information is available free of charge at https://pubs.acs.org/doi/10.1021/acsinfecdis.9b00291.

Tables S1−S4; Figures S1−S3 (PDF)

■ AUTHOR INFORMATION

Corresponding Author

*Phone: 501-686-7958. E-mail: smeltzermarks@uams.edu.

ORCID

Alan J. Tackett: 0000-0002-3672-4460

Mark S. Smeltzer: 0000-0002-0878-0692

Author Contributions

Conceived and designed the experiments: AR, KB, MS. Performed the experiments: AR, KB, SB, CW, AJ. Analyzed the data: AR, SB, CW, AJ, HS, MS. Wrote the paper: AR, KB, MS.

Notes

The authors declare no competing financial interest.

■ ACKNOWLEDGMENTS

The authors would like to acknowledge the University of Arkansas for Medical Sciences Proteomics Core Facility, Arkansas Children's Research Institute Developmental Bioinformatics Core, and the Arkansas Biosciences Institute. MSS is supported by National Institute of Allergy and Infectious Disease (NIAID) grant R01AI119380, National Institute of General Medical Sciences (NIGMS) grant P20-GM103625, Department of Defense Peer-Reviewed Orthopedic Research Program Expansion Award W81XWH-15-1-0716 (OR140356), National Institute of Arthritis and Musculoskeletal Skin Disorders (NIAMS) grant R01AR066050, the Arkansas Research Alliance, and a generous gift from the Texas Hip and Knee Center. AJT is supported by National Institute of General Medical Sciences grants P20GM121293, R01GM118760, and P20GM103429, National Center for Advancing Translational Sciences grant UL1TR000039, and National Institutes of Health Office of the Director grant S10OD018445.

■ ABBREVIATIONS

OM, osteomyelitis; *sarA*, staphylococcal accessory regulator; *saeRS*, *S. aureus* exoprotein regulatory locus; PSMs, phenol-soluble modulins; Spa, taphylococcal protein A; CM, conditioned media; μCT, microcomputed tomography; FC, fold-change; glmQLT, generalized linear model quasi-likelihood; NTML, Nebraska Transposon Mutant Library; *coa*, staphylocoagulase.

■ REFERENCES

(1) Monaco, M., Pimentel de Araujo, F., Cruciani, M., Coccia, E. M., and Pantosti, A. (2016) Worldwide Epidemiology and Antibiotic Resistance of Staphylococcus aureus. *Curr. Top. Microbiol. Immunol. 409*, 21−56.

(2) Jerzy, K., and Francis, H. (2018) Chronic Osteomyelitis - Bacterial Flora, Antibiotic Sensitivity and Treatment Challenges. *Open Orthop J. 12*, 153−163.

(3) Priest, N. K., Rudkin, J. K., Feil, E. J., van den Elsen, J. M., Cheung, A., Peacock, S. J., Laabei, M., Lucks, D. A., Recker, M., and Massey, R. C. (2012) From genotype to phenotype: can systems biology be used to predict Staphylococcus aureus virulence? *Nat. Rev. Microbiol. 10* (11), 791−7.

(4) Loughran, A. J., Gaddy, D., Beenken, K. E., Meeker, D. G., Morello, R., Zhao, H., Byrum, S. D., Tackett, A. J., Cassat, J. E., and Smeltzer, M. S. (2016) Impact of sarA and Phenol-Soluble Modulins on the Pathogenesis of Osteomyelitis in Diverse Clinical Isolates of Staphylococcus aureus. *Infect. Immun. 84* (9), 2586−94.

(5) Cassat, J. E., Hammer, N. D., Campbell, J. P., Benson, M. A., Perrien, D. S., Mrak, L. N., Smeltzer, M. S., Torres, V. J., and Skaar, E. P. (2013) A secreted bacterial protease tailors the Staphylococcus aureus virulence repertoire to modulate bone remodeling during osteomyelitis. *Cell Host Microbe 13* (6), 759−72.

(6) Beenken, K. E., Mrak, L. N., Zielinska, A. K., Atwood, D. N., Loughran, A. J., Griffin, L. M., Matthews, K. A., Anthony, A. M., Spencer, H. J., Skinner, R. A., Post, G. R., Lee, C. Y., and Smeltzer, M. S. (2014) Impact of the functional status of saeRS on in vivo phenotypes of Staphylococcus aureus sarA mutants. *Mol. Microbiol. 92* (6), 1299−312.

(7) Mrak, L. N., Zielinska, A. K., Beenken, K. E., Mrak, I. N., Atwood, D. N., Griffin, L. M., Lee, C. Y., and Smeltzer, M. S. (2012) saeRS and sarA act synergistically to repress protease production and promote biofilm formation in Staphylococcus aureus. *PLoS One 7* (6), No. e38453.

(8) Zielinska, A. K., Beenken, K. E., Joo, H. S., Mrak, L. N., Griffin, L. M., Luong, T. T., Lee, C. Y., Otto, M., Shaw, L. N., and Smeltzer, M. S. (2011) Defining the strain-dependent impact of the Staphylococcal accessory regulator (sarA) on the alpha-toxin phenotype of Staphylococcus aureus. *J. Bacteriol. 193* (12), 2948−58.

(9) Zielinska, A. K., Beenken, K. E., Mrak, L. N., Spencer, H. J., Post, G. R., Skinner, R. A., Tackett, A. J., Horswill, A. R., and Smeltzer, M. S. (2012) sarA-mediated repression of protease production plays a key role in the pathogenesis of Staphylococcus aureus USA300 isolates. *Mol. Microbiol. 86* (5), 1183−96.

(10) Gimza, B., Larias, M., Budny, B., and Shaw, L. (2019) Mapping the global network of extracellular protease regulation in Staphylococcus aureus. *bioRxiv* DOI: 10.1101/764423.

(11) Byrum, S. D., Loughran, A. J., Beenken, K. E., Orr, L. M., Storey, A. J., Mackintosh, S. G., Edmondson, R. D., Tackett, A. J., and Smeltzer, M. S. (2018) Label-Free Proteomic Approach to Characterize Protease-Dependent and -Independent Effects of sarA Inactivation on the Staphylococcus aureus Exoproteome. *J. Proteome Res. 17*, 3384.

(12) Oliveros, J. (2007) *Venny: An Interactive Tool for Comparing Lists with Venn's Diagrams.*

DOI: 10.1021/acsinfecdis.9b00291
ACS Infect. Dis. 2020, 6, 237−249

(13) McCarthy, D. J., Chen, Y., and Smyth, G. K. (2012) Differential expression analysis of multifactor RNA-Seq experiments with respect to biological variation. *Nucleic Acids Res. 40* (10), 4288−97.
(14) Robinson, M. D., McCarthy, D. J., and Smyth, G. K. (2010) edgeR: a Bioconductor package for differential expression analysis of digital gene expression data. *Bioinformatics 26* (1), 139−40.
(15) Fey, P. D., Endres, J. L., Yajjala, V. K., Widhelm, T. J., Boissy, R. J., Bose, J. L., and Bayles, K. W. (2013) A genetic resource for rapid and comprehensive phenotype screening of nonessential Staphylococcus aureus genes. *mBio 4* (1), e00537−12.
(16) Zapotoczna, M., McCarthy, H., Rudkin, J. K., O'Gara, J. P., and O'Neill, E. (2015) An Essential Role for Coagulase in Staphylococcus aureus Biofilm Development Reveals New Therapeutic Possibilities for Device-Related Infections. *J. Infect. Dis. 212* (12), 1883−93.
(17) Jin, T., Zhu, Y. L., Li, J., Shi, J., He, X. Q., Ding, J., and Xu, Y. Q. (2013) Staphylococcal protein A, Panton-Valentine leukocidin and coagulase aggravate the bone loss and bone destruction in osteomyelitis. *Cell. Physiol. Biochem. 32* (2), 322−33.
(18) Cierny, G., 3rd (2011) Surgical treatment of osteomyelitis. *Plast. Reconstr. Surg. 127*, 190S−204S.
(19) Kurtz, S. M., Lau, E., Watson, H., Schmier, J. K., and Parvizi, J. (2012) Economic burden of periprosthetic joint infection in the United States. *J. Arthroplasty 27*, 61−65.
(20) Lew, D. P., and Waldvogel, F. A. (2004) Osteomyelitis. *Lancet 364* (9431), 369−79.
(21) Kalinka, J., Hachmeister, M., Geraci, J., Sordelli, D., Hansen, U., Niemann, S., Oetermann, S., Peters, G., Loffler, B., and Tuchscherr, L. (2014) Staphylococcus aureus isolates from chronic osteomyelitis are characterized by high host cell invasion and intracellular adaptation, but still induce inflammation. *Int. J. Med. Microbiol. 304* (8), 1038−49.
(22) Szafranska, A. K., Oxley, A. P., Chaves-Moreno, D., Horst, S. A., Rosslenbroich, S., Peters, G., Goldmann, O., Rohde, M., Sinha, B., Pieper, D. H., Loffler, B., Jauregui, R., Wos-Oxley, M. L., and Medina, E. (2014) High-resolution transcriptomic analysis of the adaptive response of Staphylococcus aureus during acute and chronic phases of osteomyelitis. *mBio*, DOI: 10.1128/mBio.01775-14.
(23) Beenken, K. E., Mrak, L. N., Griffin, L. M., Zielinska, A. K., Shaw, L. N., Rice, K. C., Horswill, A. R., Bayles, K. W., and Smeltzer, M. S. (2010) Epistatic relationships between sarA and agr in Staphylococcus aureus biofilm formation. *PLoS One 5* (5), No. e10790.
(24) Claro, T., Widaa, A., McDonnell, C., Foster, T. J., O'Brien, F. J., and Kerrigan, S. W. (2013) Staphylococcus aureus protein A binding to osteoblast tumour necrosis factor receptor 1 results in activation of nuclear factor kappa B and release of interleukin-6 in bone infection. *Microbiology 159* (1), 147−154.
(25) Claro, T., Widaa, A., O'Seaghdha, M., Miajlovic, H., Foster, T. J., O'Brien, F. J., and Kerrigan, S. W. (2011) Staphylococcus aureus protein A binds to osteoblasts and triggers signals that weaken bone in osteomyelitis. *PLoS One 6* (4), No. e18748.
(26) Mendoza Bertelli, A., Delpino, M. V., Lattar, S., Giai, C., Llana, M. N., Sanjuan, N., Cassat, J. E., Sordelli, D., and Gomez, M. I. (2016) Staphylococcus aureus protein A enhances osteoclastogenesis via TNFR1 and EGFR signaling. *Biochim. Biophys. Acta, Mol. Basis Dis. 1862* (10), 1975−83.
(27) Ren, L. R., Wang, H., He, X. Q., Song, M. G., Chen, X. Q., and Xu, Y. Q. (2017) Staphylococcus aureus Protein A induces osteoclastogenesis via the NFkappaB signaling pathway. *Mol. Med. Rep. 16* (5), 6020−6028.
(28) Widaa, A., Claro, T., Foster, T. J., O'Brien, F. J., and Kerrigan, S. W. (2012) Staphylococcus aureus protein A plays a critical role in mediating bone destruction and bone loss in osteomyelitis. *PLoS One 7* (7), No. e40586.
(29) Brady, R. A., Leid, J. G., Calhoun, J. H., Costerton, J. W., and Shirtliff, M. E. (2008) Osteomyelitis and the role of biofilms in chronic infection. *FEMS Immunol. Med. Microbiol. 52* (1), 13−22.
(30) O'Neill, E., Pozzi, C., Houston, P., Humphreys, H., Robinson, D. A., Loughman, A., Foster, T. J., and O'Gara, J. P. (2008) A novel Staphylococcus aureus biofilm phenotype mediated by the fibronectin-binding proteins. *FnBPA and FnBPB. J. Bacteriol 190* (11), 3835−50.
(31) Johansson, A., Flock, J. I., and Svensson, O. (2001) Collagen and fibronectin binding in experimental staphylococcal osteomyelitis. *Clin. Orthop. Relat. Res. 382*, 241−6.
(32) Burkholder, K. M., and Bhunia, A. K. (2010) Listeria monocytogenes uses Listeria adhesion protein (LAP) to promote bacterial transepithelial translocation and induces expression of LAP receptor Hsp60. *Infect. Immun. 78* (12), 5062−73.
(33) Daniely, D., Portnoi, M., Shagan, M., Porgador, A., Givon-Lavi, N., Ling, E., Dagan, R., and Nebenzahl, Y. M. (2006) Pneumococcal 6-phosphogluconate-dehydrogenase, a putative adhesin, induces protective immune response in mice. *Clin. Exp. Immunol. 144* (2), 254−263.
(34) Jin, H., Song, Y. P., Boel, G., Kochar, J., and Pancholi, V. (2005) Group A streptococcal surface GAPDH, SDH, recognizes uPAR/CD87 as its receptor on the human pharyngeal cell and mediates bacterial adherence to host cells. *J. Mol. Biol. 350* (1), 27−41.
(35) Kim, K. P., Jagadeesan, B., Burkholder, K. M., Jaradat, Z. W., Wampler, J. L., Lathrop, A. A., Morgan, M. T., and Bhunia, A. K. (2006) Adhesion characteristics of Listeria adhesion protein (LAP)-expressing Escherichia coli to Caco-2 cells and of recombinant LAP to eukaryotic receptor Hsp60 as examined in a surface plasmon resonance sensor. *FEMS Microbiol. Lett. 256* (2), 324−32.
(36) Molkanen, T., Tyynela, J., Helin, J., Kalkkinen, N., and Kuusela, P. (2002) Enhanced activation of bound plasminogen on Staphylococcus aureus by staphylokinase. *FEBS Lett. 517* (1−3), 72−8.
(37) Wampler, J. L., Kim, K. P., Jaradat, Z., and Bhunia, A. K. (2004) Heat shock protein 60 acts as a receptor for the Listeria adhesion protein in Caco-2 cells. *Infect. Immun. 72* (2), 931−6.
(38) Kim, H. K., Thammavongsa, V., Schneewind, O., and Missiakas, D. (2012) Recurrent infections and immune evasion strategies of Staphylococcus aureus. *Curr. Opin. Microbiol. 15* (1), 92−9.
(39) Kolar, S. L., Ibarra, J. A., Rivera, F. E., Mootz, J. M., Davenport, J. E., Stevens, S. M., Horswill, A. R., and Shaw, L. N. (2013) Extracellular proteases are key mediators of Staphylococcus aureus virulence via the global modulation of virulence-determinant stability. *MicrobiologyOpen 2* (1), 18−34.
(40) Wormann, M. E., Reichmann, N. T., Malone, C. L., Horswill, A. R., and Grundling, A. (2011) Proteolytic cleavage inactivates the Staphylococcus aureus lipoteichoic acid synthase. *J. Bacteriol. 193* (19), 5279−91.
(41) Tsang, L. H., Cassat, J. E., Shaw, L. N., Beenken, K. E., and Smeltzer, M. S. (2008) Factors contributing to the biofilm-deficient phenotype of Staphylococcus aureus sarA mutants. *PLoS One 3* (10), No. e3361.
(42) Hothorn, T., Bretz, F., and Westfall, P. (2008) Simultaneous inference in general parametric models. *Biom. J. 50* (3), 346−63.
(43) Beenken, K. E., Blevins, J. S., and Smeltzer, M. S. (2003) Mutation of sarA in Staphylococcus aureus limits biofilm formation. *Infect. Immun. 71* (7), 4206−11.
(44) Beenken, K. E., Spencer, H., Griffin, L. M., and Smeltzer, M. S. (2012) Impact of extracellular nuclease production on the biofilm phenotype of Staphylococcus aureus under in vitro and in vivo conditions. *Infect. Immun. 80* (5), 1634−8.

DOI: 10.1021/acsinfecdis.9b00291
ACS Infect. Dis. 2020, 6, 237−249